

Article

City Wind Impact on Air Pollution Control for Urban Planning with Different Time-Scale Considerations: A Case Study in Chengdu, China

Jianwu Xiong¹, Jin Li² , Fei Gao³ and Yin Zhang^{1,*}¹ School of Architecture, Southwest Minzu University, Chengdu 610225, China² School of Civil Engineering, Sichuan University of Science & Engineering, Zigong 643002, China³ Sichuan Provincial Architecture Design and Research Institute, Chengdu 610000, China

* Correspondence: cdzhangyin@163.com; Tel.: +86-13488918589

Abstract: Economic development and fast growing urbanization in China have caused severe air pollution, with frequent pollution episodes endangering the health of inhabitants and disturbing social activities, and as an expanding metropolis, Chengdu has suffered ever since. The concentration variations of main air pollutants, such as PM₁₀, PM_{2.5} and NO₂, often show periodicity because of meteorological impact and anthropic activities, and display orientation discrepancies due to influences of wind speed (WS), frequency and pollutant sources. These features have complicated the mechanisms of pollution episodes and deepened the difficulty in pollution control evaluation. The WS has significant influences on the periodicity and orientation variations in pollutant concentrations, and quantifying the influence of which is of high significance and provides sustainable foundations for pollution alleviation strategies. Different time-scale cycles (i.e., Diurnal, weekly, seasonal and annual), along with the WS, wind frequency, wind and spatial orientations in urban areas, were analyzed in this paper. Results show that the periodicity of diurnal, seasonal and annual cycles is remarkable, and weekly cycle is obvious by adding the influence of the WS in 16 orientations. The WS has direct impacts on pollutants varying in the range of 1.5–2.5 m/s, and has a remarkable diffusion effect on pollutants once above 2.5 m/s. Over heavy pollution hours in diurnal, weekly, annual cycles and transitional seasons, the WS had more significant influences on pollutants, and whereas the wind frequency is not the main impact factor for orientation variations. For Chengdu, the northeast orientation is suitable to construct a wind panel with a remarkable diffusion effect on pollutants, while air pollutions in the northwest and southwest orientations were severe with the WS below 1.5 m/s, and pollution diffusion in the north-northwest orientation was the worst. This work can provide guidance and reference for urban planning optimization and air environment protection in cities with air quality control considerations impacted by city wind.

Keywords: city wind; air pollutants; orientation variations; concentration; urban planning

Citation: Xiong, J.; Li, J.; Gao, F.; Zhang, Y. City Wind Impact on Air Pollution Control for Urban Planning with Different Time-Scale Considerations: A Case Study in Chengdu, China. *Atmosphere* **2023**, *14*, 1068. <https://doi.org/10.3390/atmos14071068>

Academic Editors: Sumei Liu, Junjie Liu and Wei Liu

Received: 29 May 2023

Revised: 17 June 2023

Accepted: 22 June 2023

Published: 24 June 2023



Copyright: © 2023 by the authors. Licensee MDPI, Basel, Switzerland. This article is an open access article distributed under the terms and conditions of the Creative Commons Attribution (CC BY) license (<https://creativecommons.org/licenses/by/4.0/>).

1. Introduction

With the rapid economic achievement and development in China, accelerated urbanization has been catalyzing many megacities like Chengdu, serving as one of the national central cities in western China [1]. Urban features affect the atmospheric flow, turbulence regime, circulation and microclimate, by means of the UHI (Urban heat island), increased surface roughness, and concentrated condensation nuclei by which the PMs (particulate matters) can be transformed into aerosols [2]. With the population and resources clustering in expanding urban sprawls, the high density implies more severe emissions, pollution concentrations and population exposures [3]. In addition, it has multiple impacts on the health of inhabitants, and few threats are more fiercely felt by residents than air pollution [4]. With recent years' high frequencies of air pollution episodes in China, the air

quality deterioration and PM concentration phenomenon have become one of the priorities of public concerns [5]. Anthropogenic emissions, formation of secondary aerosol and adverse meteorological conditions are considered as main causes of heavy pollution episodes, which are often related to stagnant dispersion conditions, and measures are needed urgently to alleviate the air pollution in response to short-term alerts.

Recent studies on heavy pollution episodes emphasized the combination of observation and numerical simulation to visualize the influences of multiple meteorological factors on haze events, which are mainly concerned with large spatial areas and short time intervals [6]. Other studies focused on special time ranges, such as monsoon seasons, abnormal weather events and festivals, and either the meteorological or anthropogenic influence on pollutants was emphasized, but studies referring to the comprehensive effect of the two were few [7]. For data scales and time ranges, daily or monthly samples were common for studies referring to annual or yearly ranges, while studies involving hourly data were often related to the field measurement, which usually lasted for days or weeks, but very few can extend data scales to 8760 h over the year [8]. Moreover, studies on air pollution control measures focused on restricting pollutant sources, which was a fundamental solution to eradicate air pollution, but the effect of which that performed in the long term was difficult to be evaluated, since short-term meteorological influences on pollutants were remarkable and often concealed original effects of emission control measures [9,10]. Improving urban planning strategy based on wind distribution for ventilation can lessen the intensity of pollution episodes instantly, and short-term changes in atmospheric stability would exert more considerable impacts on urban pollutants than control source strengths, hence researching the periodicity of the wind environment and pollutant variations can optimize pollution control strategies and its evaluation methods [11].

Air pollution in Chengdu has specific sources, and among pollution episodes recently, the low fluidity and temperature inversion phenomena were meteorological symbols of secondary pollution events, while the long-range transport source was the main cause of dust events [12]. Chen et al. [13] analyzed two dust events in 2013 and found that the desert dust air in Chengdu was mostly from the northeast and strongly impacted the local air quality, but exhibited weak regional features. Shi et al. [14] indicated that higher contributions of the crustal dust in spring were caused by strong winds, and found that nightly winds cleared many of the pollutants from the air shed, and had no noticeable weekday/weekend effect. Wang et al. [15] compiled the air pollutant emission inventory of Chengdu, according to the Multiresolution Emissions Inventory of the Chinese Model, 2017 (MEIC v1.3), and found that the pollutant emission of Chengdu is generally higher in winter than in summer, emissions of residential and industrial sectors are dominant. Zhou et al. [16] completed the IVE model and calculated the motor vehicle emission factors on various types of roads in Chengdu's different development areas, the spatial distribution of on-road mobile source pollutant emissions showed that emissions were concentrated in the downtown with a decreasing trend from the downtown to the suburbs and the outer suburbs. Hu et al. [17] based on land-use (LU) classification maps, examined the effects of urban landscapes on pollutant concentrations at different spatial and temporal scales in Chengdu and found that increasing the area, largest patch index, and patch cohesion of forests and grasslands, as well as reducing the area, largest patch index, and patch cohesion of farmlands and developed lands, could effectively lower pollutant concentrations. Wang et al. [18] assessed the effects of extensive usage of air conditioning systems in Chengdu during summertime, and the results suggest that using air conditioning systems facilitates the dispersion of air pollutants over Chengdu. Sun et al. [19] used GIS spatial analysis technology and landscape ecology analysis methods to analyze the dynamic changes in land cover and landscape patterns in Chengdu as a result of urban development, evaluated and compared the wind speed and temperature results simulated using new and old land-use data (1980 and 2015), the results show that the concentration of PM_{2.5} in urban areas was higher than that in the suburbs, and the concentration of PM_{2.5} was lower on Longquan Mountain in Chengdu than in the surrounding areas. The above studies were

involving meteorological simulations, pollutant variations and sources in Chengdu, but results had limited significance in instructing short-term pollution control, and orientation variations in pollutant concentrations were still indistinguishable, and quantified analyses on proper wind conditions in alleviating the air pollution were also in deficiency [20,21].

The wind can both dilute and transport pollutants, but the weak surface wind and low mixing layers would limit the dispersion of urban pollutants, and anomalous winds in the lower troposphere may transport external sources [22]. The wind speed (WS) was thought to be inversely sensitive to pollutants, and airborne concentrations attributed largely to the dispersion prompted by the WS. Grundström et al. [23] found that the low WS was common in some Lamb Weather Types with specific prevailing wind directions, and concluded that both concentrations and size distributions of the PM were strongly dependent on the meteorological conditions, with the wind direction as the dominant influencing factor. Squizzato et al. [24] found that the high WS can reduce pollutant concentrations by increasing the vertical dispersion, but can also transfer pollutants from a buoyant source. Uria-Tellaetxe et al. [25] concluded that negative correlations between aerosol mass concentrations and the WS indicate the dominance of local sources, and found that different source types can have different WS dependencies. The above studies were involving cities that are mostly located in coastal areas, which are often affected by monsoons and sea winds [26]. While for cities in the hinterland like Chengdu, high still wind frequencies were common but received limited attention [27]. A study in Shenzhen, a mega city in southern China, has confirmed that the urban surface-wind patterns greatly affected pollutant concentrations [28]. The above results proved the influences of the wind direction and WS on pollutants separately, but neglecting the combined effect of the two, and ignoring orientation variations in pollutant concentrations that were affected by the WS and discrepant spatial allocations [29]. Thus, clarifying local ventilation patterns and quantifying the proper wind condition in prompting pollutant dispersion are of high significance to assess the effect of source control strategies and short-term pollution episodes, which might have a profound and long-run beneficial influence on public health with exposure risk control of main city air pollutants [30,31].

The main objective of this research is to quantify the alleviation effect of urban ventilation on air pollution from perspectives of both time and space and provide guidance for pollution control strategies. The influence of the WS on pollutants at multiple time scales can be analyzed by introducing the periodicity in 4 cycles, and orientation variations in pollutant concentrations can be judged by referring to wind and spatial orientations. Influences of the WS on the PM₁₀, PM_{2.5} and NO₂ concentrations contain the interference of the pollutant transportation and the alteration of the diffusion effect. Moreover, the causes of the heavy pollution status, rather than the non-directional pollutant sources, can be further analyzed by identifying orientation variations of pollutants. The urban space is divided into 16 orientations, and the pollutant concentrations in each orientation are analyzed superimposed on the distribution of urban land and important public infrastructure. This study identifies the main land use types in heavily polluted areas of the city and explores the main causes of pollution in different areas of the city, and analyzes the relationship between urban spatial characteristics and the dispersion of PM₁₀, PM_{2.5} and NO₂ pollutants. The conclusions can provide information for cities to develop pollution reduction strategies for different areas. In addition, valuable wind panels in urban areas can be identified by considering the wind environment and local pollution status. This work is important for pollution control measures optimization in the short and middle term in tackling heavy pollution episodes, by analyzing heavy pollution hours in 4 cycles and the effect of the WS and anthropogenic patterns on the air quality, and proposing a feasible standard to evaluate the rationality of urban allocations, by analyzing orientation variations of pollutants in the spatial dimension. The used analysis method is general, which can be applied to other cities that with limited wind resources (e.g., those located in the hinterland), and have illustrative significance in delving into the effect of the wind environment and urbanization on the air quality. This work can provide guidance and

reference for urban planning optimization and air environment protection in cities with air quality control considerations impacted by city wind.

2. Methods

2.1. Geographical Information of Chengdu City

Chengdu, one of the biggest inland metropolises in southwestern China, is located at 102.9° E–104.9° E in longitude and 30.1° N–31.4° N in latitude and is the capital of Sichuan province. Within the range of the Chengdu plain (12,390 km²), the planning control area of the central city is 626 km², Chengdu covers a built-up area of 2176 km² and occupies the western part of the Sichuan basin, which is surrounded by the Tibetan plateau in the west, Yunnan-Kweichou Plateau in the south and Qin Mountain range in the north. Chengdu is nearly free of exterior incursions due to its topography, and has a subtropical monsoon climate with high frequencies of still wind, and hours with the condition of “no wind” and “indefinite wind direction” occupies more than half of the year (details in Table 1). According to the textual information of the “General Land Use Plan of Chengdu (2006–2020)”, the urbanization of the central city of Chengdu shows a trend of expansion to the northwest and south, and its construction land and building density are growing rapidly. The northwestern part of the central city is a cluster of industries such as industrial and mining industries and logistics industries, as well as a rail transportation hub area that connects to other cities in western China. The southern part of the central city is a high-tech industry cluster and is an important area for Chengdu to connect to global air transportation. The center area is dominated by residential land and public facilities. The eastern part of the city was once the old industrial area of Chengdu, but after a series of old city renovation measures such as industrial restructuring and people’s welfare projects, it has become the main recreational area of the city, with the highest amount of concentrated green space. Satellite cities in the outskirts have specific functions: Pidu district concentrates on industries, Wenjiang functions as the technology and innovation center, Shuangliu country serves as the air transport center, Longquanyi lay emphases on automobile manufacturing, and Xindu sets goals for freight transport. Tianfu’s new district includes the Wuhou, Chenghua districts and Shuangliu districts, and will be the new city center with large amounts of construction (including the new Tianfu International Airport).

Table 1. 11 groups in diurnal, weekly, seasonal and annual cycles.

	Clusters	Time Ranges	Hours		Clusters	Details	Time Ranges	Hours		
Diurnal cycle	Peak hours	24:00~11:00	4380	Annual Cycle	Festival hours	New Year’s Day	00:00, 1 January 2019~23:00, 3 January 2019	72		
	Off-peak hours	12:00~23:00	4380			Spring Festival	00:00, 7 February 2019~23:00, 13 February 2019	168		
Weekly cycle	Weekday hours	00:00, Monday~23:00, Friday	6240			Tomb Sweeping Day	00:00, 2 April 2019~23:00, 4 April 2019	72		
	Weekend hours	00:00, Saturday~23:00, Sunday	2520			May Day	00:00, 30 April 2019~23:00, 2 May 2019	72		
Seasonal cycle	Winter hours	00:00, 19 December 2018~23:00, 3 February 2019	2112			Dragon Boat Festival	00:00, 9 June 2019~23:00, 11 June 2019	72		
		00:00, 7 November 2019~23:00, 17 December 2019				Mid-autumn Festival	00:00, 15 September 2019~23:00, 17 September 2019	72		
	Spring hours	00:00, 4 February 2019~23:00, 4 May 2019	2184			National Day	00:00, 1 October 2019~23:00, 7 October 2019	168		
	Summer hours	00:00, 5 May 2019~23:00, 5 August 2019	2232			TRD hours	Spring Festival Rush	00:00, 24 January 2019~23:00, 3 March 2019	977	
Autumn hours	00:00, 6 August 2019~23:00, 6 November 2019	2232	Summer Holiday Rush				00:00, 1 July 2019~23:00, 31 August 2019	1487		
						Workday hours				5600

2.2. Meteorological Data

Data of the wind orientation and frequency, WS, PM₁₀, PM_{2.5} and NO₂ concentrations for over 8760 h were collected in this paper, covering hourly variations from 2018.12.19 to 2019.12.18. Real data of the wind orientation and WS were assembled from the meteorological monitor (Figure 1) that was set by the airport, with consecutive updating by the website. Three pollutants were monitored by the local environmental protection department, and released by the Chengdu environmental air quality publishing system. The air quality monitor of “Wuhou technical park” was selected since it lies between the meteorological monitor and the city center, and can lessen the excessive interferences between the vehicle traffic and the UHI. PM₁₀, PM_{2.5} and NO₂ are major pollutants locally and often exceed the national air quality standard. NO₂ is a gaseous pollutant and mainly originated from vehicle exhaust and agricultural chemicals, and is one of the major sources of the UFP (Ultra-fine particle) which includes PM₁₀ and PM_{2.5}. The lifetime of the NO₂ is rather short and can be the indicator for the real time variation and local pollutant source, whereas the PM₁₀ and PM_{2.5} have lifetimes of about 1–2 weeks and months, and can be indicators for long range transport sources.

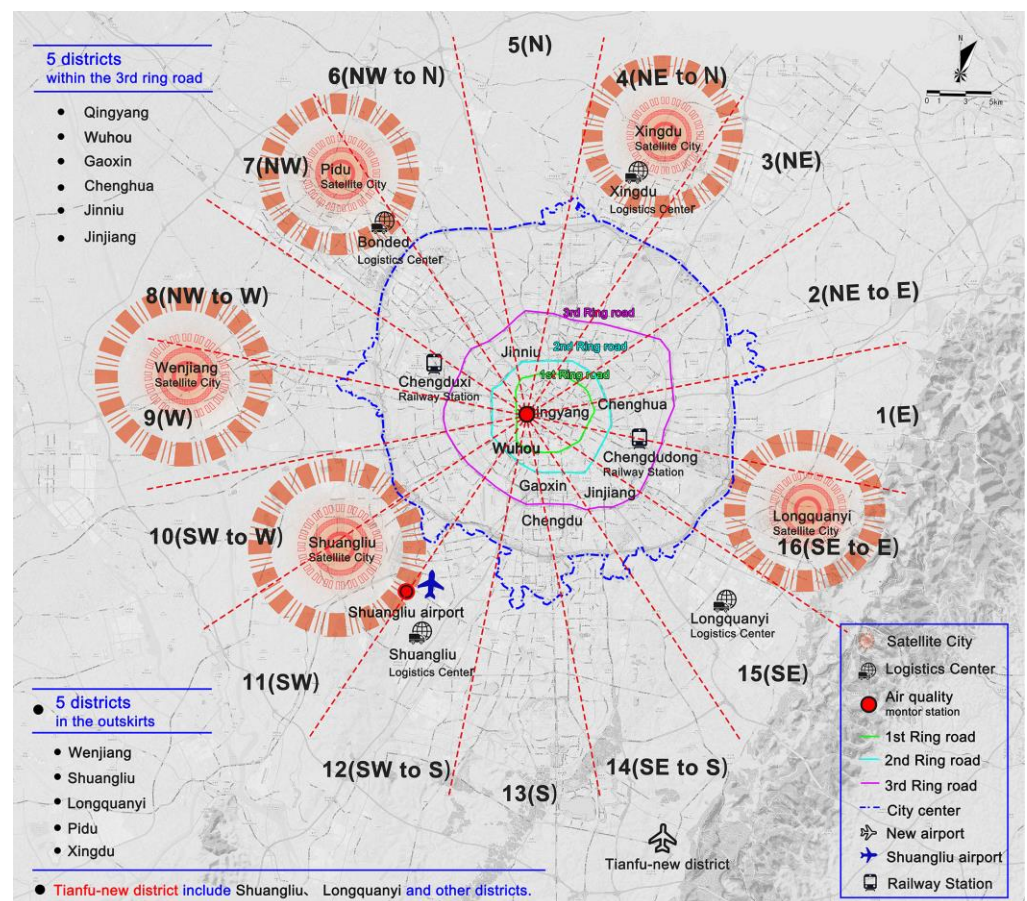


Figure 1. Wind and spatial orientations of Chengdu and the location of monitors and satellite cities.

Data of 8760 h were classified into different groups, 24 h in a day, 7 days in a week, 3 months in a season, official festival, travel-rush-day (TRD) and workday in a year, based on the periodicity of diurnal, weekly, seasonal and annual cycles accordingly (Table 1). The diurnal cycle can be further divided into the peak and off-peak hours in terms of fluctuant features of the WS and 3 pollutants in a day, with dividing points at 11:00 and 23:00. Weekly cycle can be divided into the weekday (from Monday to Friday) and weekend (Saturday and Sunday) hours, covering 6240 h and 2520 h individually. The dividing points in the seasonal cycle corresponded to the Chinese lunar calendar: spring begins

(19 February 2004), summer begins (19 May 2005), autumn begins (19 August 2006) and winter begins (19 November 2007), and each season corresponded to 3 months. According to the official festival and TRD schedule, the annual cycle can be divided into festival, TRD, and workday hours. Above all, hourly data of 11 clusters in 4 cycles showed the comprehensive effect of the meteorology and anthropogenic patterns, and heavy pollution hours can be distinguished by comparisons.

To further analyze orientation variations of the WS and 3 pollutants, 16 wind and spatial orientations (Figure 1) were introduced in Chapter 4. Hours in 11 clusters can be further classified into 16 orientations (Table 2), by precluding hours of “no wind” and “indefinite direction”, and mean values of the WS and pollutant concentration can be calculated according to 16 orientations. The wind frequency of 16 orientations had two groups of peak values: the group of “NE to N” (4), “N” (5) and “NW to N” (6), and the group of “SW” (11), “SW to S” (12) and “S” (13), with the orientation “N” (5) had the maximum frequency, and orientation “SW to S” (12) was second to that; and the group of “NW” (7), “NW to W” (8) and “W” (9) was the valley value, with “NW to W” (8) had the minimum frequency, and “W” (9) was second to that. The orientation with higher wind frequency had better utilization value and can enhance the dispersion of pollutants by constructing wind panels, while the orientation with lower wind frequency should be cautious of nearby pollutant sources.

Table 2. Wind frequencies of 16 orientations in 11 groups.

	No Wind		Indefinite Direction		16 Orientations																	
	Hour	%	Hour	%	SUM	E (1)	NE to E (2)	NE (3)	NE to N (4)	N (5)	NW to N (6)	NW (7)	NW to W (8)	W (9)	SW to W (10)	SW (11)	SW to S (12)	S (13)	SE to S (14)	SE (15)	SE to E (16)	
	Hour	%	Hour	%	Hour	%	Wind Frequency (%)															
Peak Hours	1568	36%	1106	25%	1706	39%	1.29	1.70	3.17	5.98	21.9	10.0	2.75	0.70	1.47	5.51	11.6	16.5	9.96	3.99	2.17	1.29
Off-peak Hours	577	13%	1176	27%	2627	60%	4.30	4.00	4.76	10.8	19.1	6.66	2.13	0.84	1.37	3.05	7.96	12.0	10.7	4.11	3.81	4.45
Weekday Hours	1542	25%	1670	27%	3028	49%	3.27	3.10	4.39	8.49	20.7	8.39	2.48	0.76	1.62	3.90	9.58	13.1	10.1	3.76	2.91	3.43
Weekend Hours	603	24%	612	24%	1305	52%	2.76	3.07	3.52	9.89	18.9	7.05	2.15	0.84	0.92	4.29	8.97	15.3	11.2	4.75	3.75	2.68
Winter hours	573	27%	589	28%	950	45%	5.05	3.37	4.42	10.0	20.2	8.74	1.79	0.63	0.84	2.74	9.58	12.2	9.89	4.42	2.53	3.58
Spring hours	586	27%	545	25%	1053	48%	4.75	3.23	5.22	10.3	19.6	7.31	2.09	1.14	2.37	4.65	10.9	10.7	7.41	3.13	3.32	3.89
Summer hours	419	19%	578	26%	1235	55%	1.38	2.43	3.97	7.21	18.6	8.66	2.75	0.73	1.30	4.86	8.26	15.4	13.8	5.18	2.91	2.59
Autumn hours	567	25%	570	26%	1095	49%	1.83	3.47	3.01	8.58	22.5	7.21	2.74	0.64	1.10	3.56	9.04	16.3	9.95	3.38	3.84	2.92
Festival hours	193	28%	147	21%	356	51%	3.09	2.25	3.93	8.99	20.5	8.15	2.53	1.12	0.56	2.53	8.71	14.9	11.5	3.37	5.34	2.53
TRD hours	706	29%	638	26%	1120	45%	2.95	3.48	2.86	5.71	17.4	10.3	2.95	0.98	1.79	3.48	8.48	15.0	11.1	5.54	4.38	3.66
Workday hours	1352	24%	1422	25%	2826	50%	3.08	3.04	4.67	10.2	21.2	6.86	2.12	0.67	1.38	4.35	9.91	13.2	10.1	3.61	2.44	3.08

3. Results

3.1. Pollutant Concentrations and WS in Diurnal, Weekly, Seasonal and Annual Cycles

Figure 2 shows the average curves and fluctuation ranges of 3 pollutants and the WS in the diurnal cycle, and the PM₁₀ concentration was the highest with wider fluctuation ranges in 24 h and per hour, while the NO₂ concentration was close to the PM_{2.5} concentration but with smaller fluctuations in per hour. In the diurnal cycle, the period from 23:00 to 11:00 was defined as peak hours, during which pollutant concentrations were high and remained almost unchanged; while the period from 11:00 to 23:00 was defined as off-peak hours, and showed apparent valleys in three curves. The bar graph showed variations of the WS, with average values fluctuating around 1.85 m/s in peak hours and 1.05 m/s in off-peak

hours, with average values varying from 0.7 m/s to 2.3 m/s. In peak hours, the PM_{10} and $PM_{2.5}$ curves were moderate and average values fluctuated around $120 \mu\text{g}/\text{m}^3$ and $75 \mu\text{g}/\text{m}^3$ respectively, while the NO_2 curve had a small valley and average values varied from $60 \mu\text{g}/\text{m}^3$ to $80 \mu\text{g}/\text{m}^3$. In off-peak hours, apparent valleys occurred in 3 curves, which may concern higher WS and escalating temperature in the afternoon, and average values of the PM_{10} , $PM_{2.5}$ and NO_2 varied from $80 \mu\text{g}/\text{m}^3$ to $117 \mu\text{g}/\text{m}^3$, from $50 \mu\text{g}/\text{m}^3$ to $70 \mu\text{g}/\text{m}^3$, and from $42 \mu\text{g}/\text{m}^3$ to $80 \mu\text{g}/\text{m}^3$, respectively. Moreover, as NO_2 has close relationships with vehicle exhausts, two peaks in the diurnal cycle indicated the morning and evening travel rush hours, but with delays for 2 or 3 h. The average curves of the three pollutants showed different patterns in peak and off-peak hours, and the periodicity of the diurnal cycle was obvious.

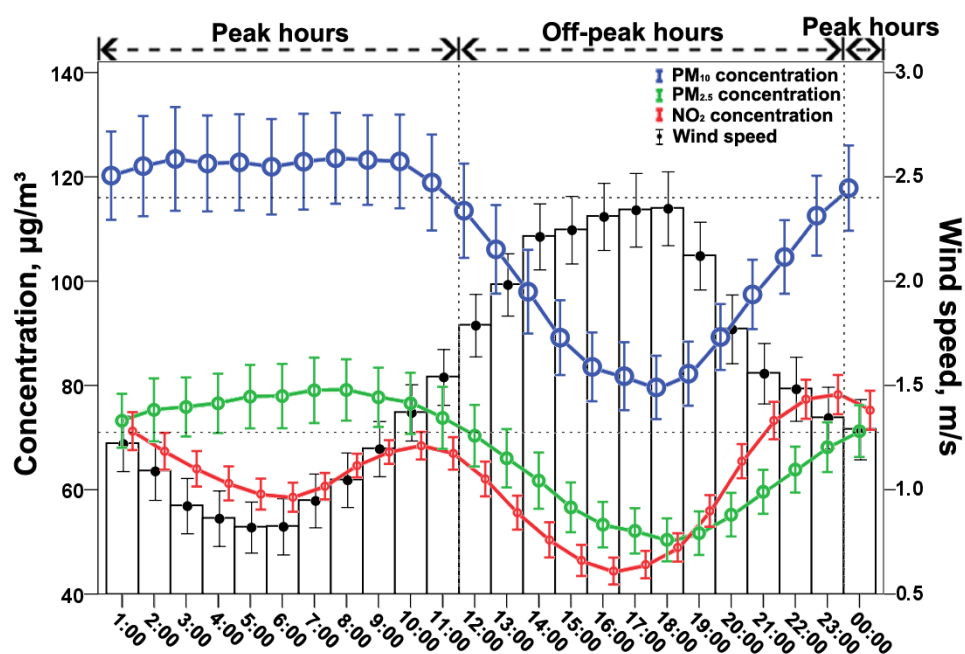


Figure 2. Pollutant concentrations and the WS in diurnal cycle.

Average values and fluctuation ranges of three pollutants and the WS for over seven days per week were shown in Figure 3, and weekday hours included hourly data from Monday to Friday, while weekend hours indicated hours on Saturday and Sunday. The PM_{10} concentration was the highest with wider fluctuation ranges daily and in seven days, while the NO_2 concentration was the lowest with narrow fluctuation ranges. Average values of the PM_{10} and $PM_{2.5}$ fluctuated around $115 \mu\text{g}/\text{m}^3$ and $75 \mu\text{g}/\text{m}^3$, respectively, while the NO_2 concentration was above $64 \mu\text{g}/\text{m}^3$ during weekday hours and below that during weekend hours, which indicated the traffic decrease during the weekend. Moreover, pollutant concentrations were higher on Monday, apart from smaller WS, indicating that air pollution was more severe at the beginning of the workday. PM_{10} and $PM_{2.5}$ concentrations were the lowest on Wednesday, but the NO_2 concentration was the highest, and the apparent low WS indicated stagnant dispersion conditions, which can be ascribed to local pollutant sources other than exterior sources. Above all, pollutant concentrations had small peak-valley differences in seven days with no more than $10 \mu\text{g}/\text{m}^3$, and the average WS varied in the range between 1.4 m/s and 1.55 m/s, and there were no apparent discrepancies in weekday and weekend hours, and the periodicity of the weekly cycle was vague.

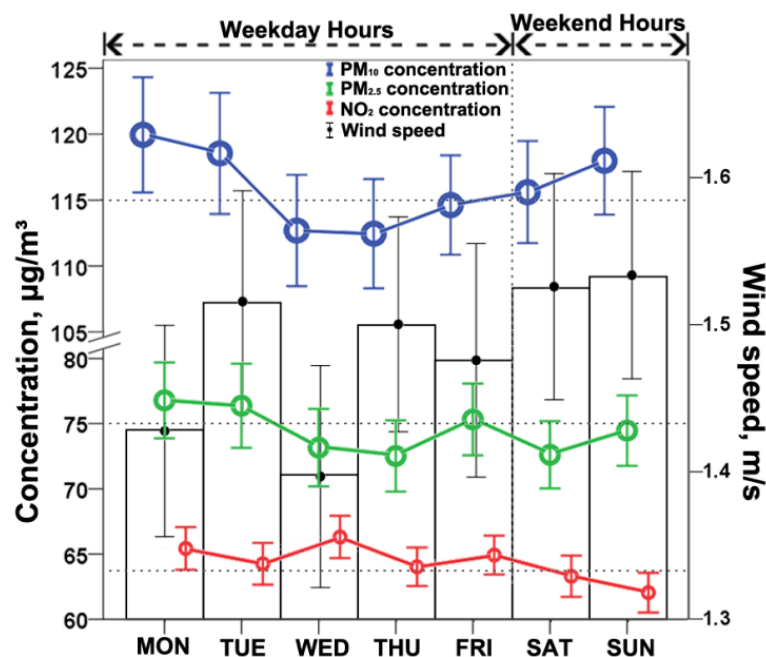


Figure 3. Pollutant concentrations and the WS in weekly cycle.

Figure 4 showed average curves and fluctuation ranges of three pollutants and the WS in 12 months, and every three months corresponded to one season. The PM₁₀ concentration was the highest with a wider fluctuation range in each month and per season, while the NO₂ concentration was close to the PM_{2.5} concentration but with a smaller fluctuation. Pollutant concentrations showed that: winter hours > spring hours > autumn hours > summer hours, and average curves of three pollutants had the biggest variations in winter hours and smallest variations in spring hours. PM₁₀, PM_{2.5} and NO₂ concentrations obtained peak values in December, which were 215 µg/m³, 160 µg/m³ and 85 µg/m³, respectively, and with subsequent decreases for months; and after obtained valley values in July, which were 65 µg/m³, 42 µg/m³ and 50 µg/m³, average curves were escalating. Aberrant values occurred in March, PM₁₀ and NO₂ concentrations were apparently higher than average curves by reaching 145 µg/m³ and 80 µg/m³, and except for the higher WS and better dispersion effect. These phenomena might be related to exterior sources or the late spring coldness. WS variations in the bar graph showed the opposite trend with pollutant concentrations basically but not in the good coupling since influences of other meteorological factors on pollutants could be in-negligible. Average WS obtained the highest value of 1.85 m/s in May and obtained the lowest value of 1.07 m/s in December, and aberrant values occurred in February and September (both were 1.35 m/s). Above all, the periodicity in the seasonal cycle was obvious.

Festival, TRD and workday hours were distributed over the year, and were inappropriate to demonstrate by temporal sequence, thus box-whisker plot graphs in Figure 5 indicated average values and fluctuation ranges of three pollutants and the WS in the annual cycle. In festival hours, PM₁₀ and PM_{2.5} concentrations had the highest average values, which were 115 µg/m³ and 90 µg/m³, respectively, and had the widest fluctuation ranges, with the lower and upper quartiles being 85 µg/m³ and 170 µg/m³ for PM₁₀ concentrations and were 50 µg/m³ and 115 µg/m³ for PM_{2.5} concentrations. During workday hours, the average value of the NO₂ concentration was the highest (70 µg/m³). In TRD hours, PM₁₀, PM_{2.5} and NO₂ concentrations had the lowest average values which were 90 µg/m³, 50 µg/m³ and 55 µg/m³, respectively, and had the narrowest fluctuation ranges, with the lower and upper quartiles were 55 µg/m³ and 115 µg/m³ for PM₁₀ concentrations, and were 33 µg/m³ and 73 µg/m³ for PM_{2.5} concentrations, and were 30 µg/m³ and 70 µg/m³ for NO₂ concentrations. The average WS in Festival, TRD and workday hours were all 1 m/s, and the WS in festival hours had wider fluctuation ranges. Above all, air

quality was bad during festival hours, and the abrupt increase in festival activities was the main cause of deterioration. Pollutant concentrations in TRD hours were significantly lower, with the decrease of pollutant sources, and were also related to the pervasive of rail transit. With discrepancies in the festival, TRD and workday hours, the periodicity in the annual cycle was obvious.

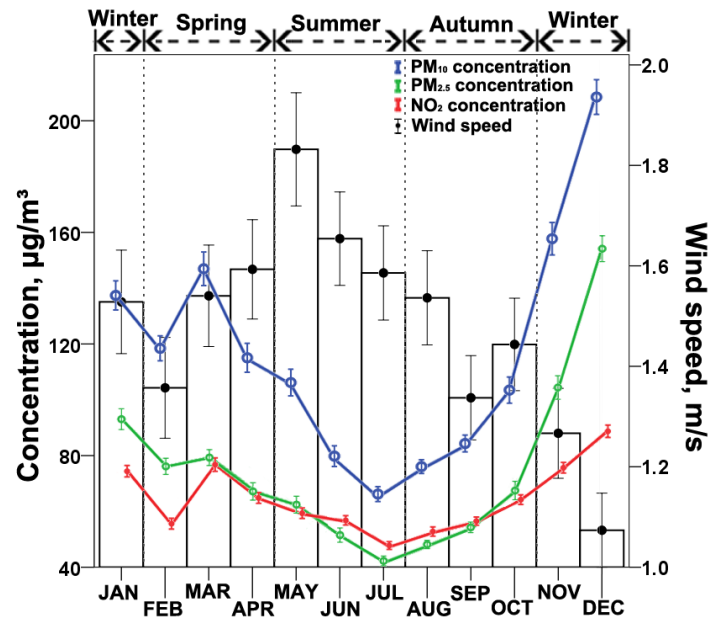


Figure 4. Pollutant concentrations and the WS in seasonal cycle.

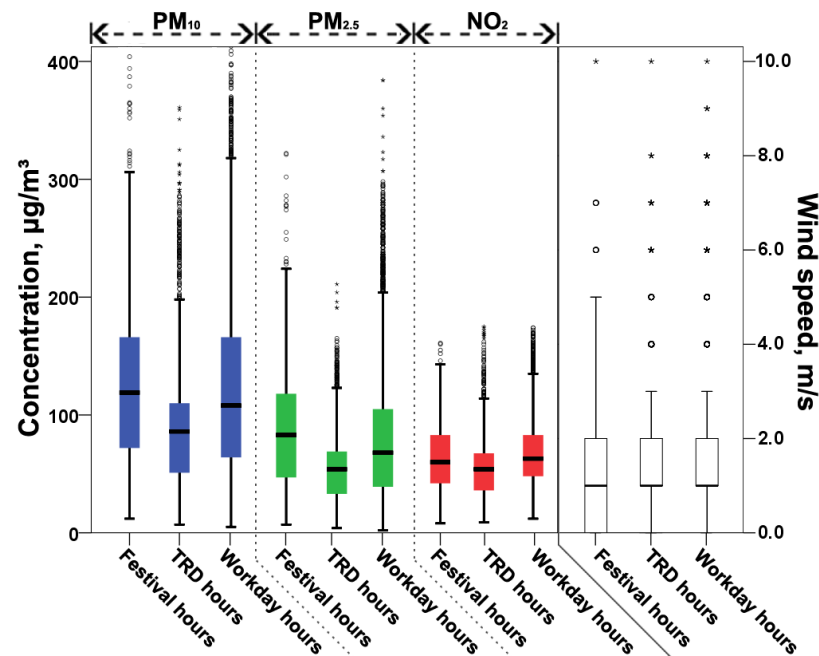


Figure 5. Pollutant concentrations and the WS in annual cycle: Box-whisker plots of PM₁₀ (blue), PM_{2.5} (green) and NO₂ (red) concentrations and the WS (white). The lower and upper ends of the boxes signify lower and upper quartiles, respectively, and the short lateral lines inside the boxes indicate the mean values. The lengths of whisker denote the 5–95% range, and the star (*) marks the aberrant values.

3.2. Influence of WS on Pollutant Concentrations in 16 Orientations

The influence of the WS on pollutant concentrations was demonstrated by linear equations with data points that corresponded to 16 orientations. It indicates that pollutant concentration always decreases with increasing WS. Figure 6 shows (a) peak and (b) off-peak hours in the diurnal cycle, and the linear R^2 between the WS and PM_{10} , $PM_{2.5}$ and NO_2 concentrations in peak hours, which were 0.791, 0.784 and 0.803, respectively, were higher than that in off-peak hours, with values were 0.413, 0.343 and 0.555. In the diurnal cycle, the WS had a greater effect on the NO_2 concentration than on the PM_{10} and $PM_{2.5}$ concentrations, and pollutant concentrations in peak hours were higher than that in off-peak hours. During peak hours, the WS had significant influences on three pollutants, illustrating that as the WS prompted the dispersion of pollutants, exterior sources were also introduced. While in off-peak hours, the WS had limited influences on three pollutants and pollutant concentrations were basically affected by local pollutant sources. Moreover, when the WS varied in the range of 1.5–2.5 m/s, linear correlations between the WS and three pollutants were significant, illustrating that the WS had direct impacts on pollutants, and aberrant values occurred once beyond that range. Furthermore, PM_{10} and $PM_{2.5}$ concentrations that corresponded to the orientation “NE to E” (2) in Figure 6a were below average levels, and pollutant concentrations that corresponded to the orientation “NW to W” (8) in Figure 6b were far above average levels.

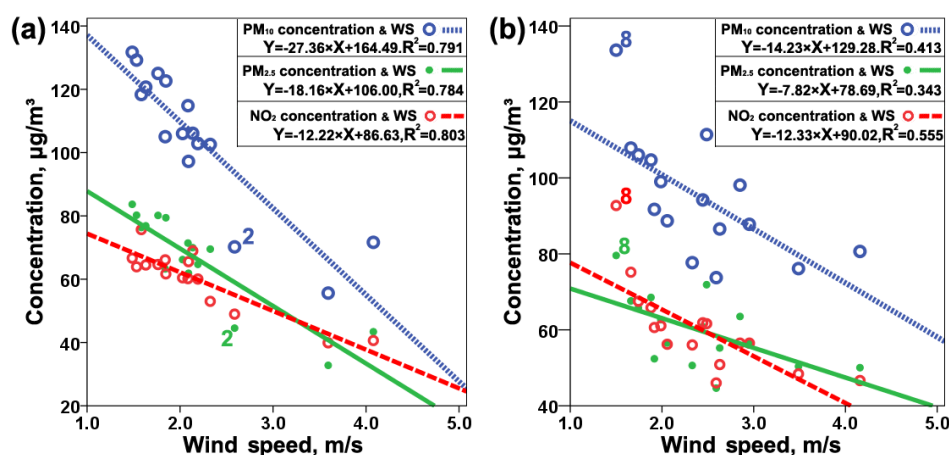


Figure 6. Influence of WS on pollutant concentrations over (a) diurnal peak and (b) off-peak hours.

Figure 7 showed comparisons between (a) weekday and (b) weekend hours, and pollutant concentrations in the weekly cycle had no obvious discrepancies, but the linear R^2 between the WS and PM_{10} , $PM_{2.5}$ and NO_2 concentrations in weekday hours (R^2 is 0.744, 0.682 and 0.64) were apparently higher than that in weekend hours (R^2 is 0.44, 0.526 and 0.592). During weekday hours, influences of the WS on three pollutants were significant and the WS had a greater effect on PM_{10} concentration than on NO_2 concentration, while in weekend hours, WS had limited influences on three pollutants. The periodicity of the weekly cycle was vague when judged by pollutant concentrations, but can be significant by considering the influence of the WS on three pollutants. Moreover, disparities of the R^2 between the WS and NO_2 concentration during weekday and weekend hours were slight, thus during weekend hours, when the influence of the WS on PM_{10} and $PM_{2.5}$ decreased, the WS seemed to have a greater effect on NO_2 . This phenomenon indicated source discrepancies of three pollutants in the weekly cycle: during weekday hours, three pollutants had steady sources both locally and exteriorly; while during weekend hours, the influence of the WS on PM_{10} and $PM_{2.5}$ concentrations decreased significantly and the WS had no apparent decrement, illustrating that pollutant sources of UFP were unsteady, which largely affected by anthropogenic activities. Furthermore, the WS concentrated in the range of 1.5–3 m/s in the weekly cycle, and the NO_2 concentration that corresponded

to the orientation “NW to W” (8) in Figure 7a was far beyond the average level with the WS below 1.5 m/s.

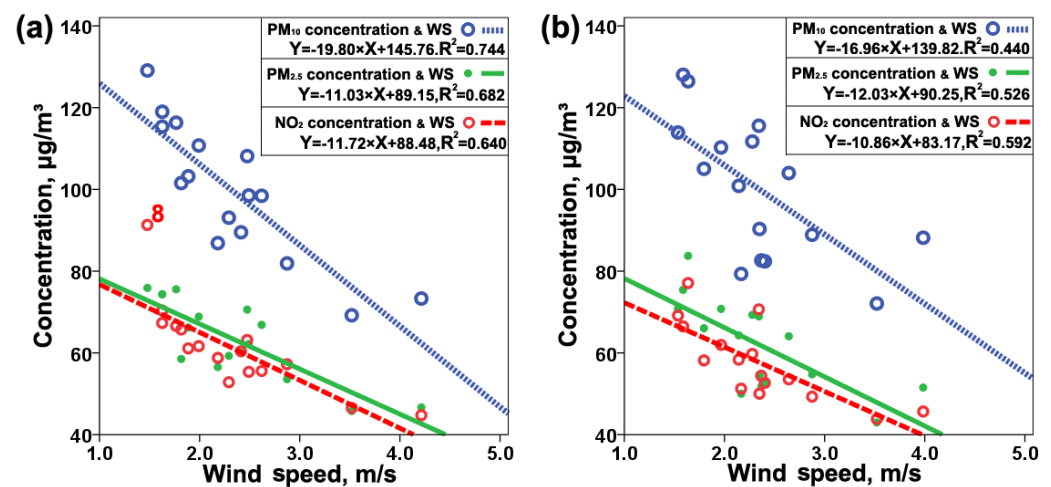


Figure 7. Influence of WS on pollutant concentrations over (a) weekday and (b) weekend hours.

Figure 8 showed (a) winter, (b) spring, (c) summer and (d) autumn hours in the seasonal cycle, and the linear R^2 between the WS and PM₁₀, PM_{2.5} and NO₂ concentrations in transitional seasons (R^2 is 0.648, 0.692 and 0.7 in spring hours, and were 0.711, 0.693 and 0.479 in autumn hours) were higher than that in winter (R^2 were 0.519, 0.443 and 0.618), while the R^2 in summer hours were the lowest. Pollutant concentrations were the highest in winter hours, and the WS had a greater effect on the NO₂ concentration than on the PM_{2.5} concentration; while in summer hours, pollutant concentrations were the lowest, and the WS had limited influences on three pollutants. Moreover, compared to spring hours, the WS had a far more significant influence on the PM₁₀ concentration than on the NO₂ concentration in autumn hours, illustrating that significant long range transport sources existed in autumn hours; while in spring hours, the influential extent of the WS on three pollutants were in equilibrium and pollutant concentrations were affected by local and exterior sources. Furthermore, PM₁₀ and PM_{2.5} concentrations that corresponded to orientation “W” (9) in Figure 8a were far below average levels, resulting in a low overall R^2 in winter hours. In transitional seasons, when WS varied in the range of 1.5–2.5 m/s, linear correlations with three pollutants were more significant.

Figure 9 showed the (a) festival, (b) TRD and (c) workday hours in the annual cycle, and the linear R^2 between the WS and PM₁₀, PM_{2.5} and NO₂ concentrations in workday hours (R^2 were 0.685, 0.639 and 0.719) were higher than that in festival hours (R^2 is 0.44, 0.601 and 0.7), while the R^2 in TRD hours were the lowest. Pollutant concentrations were the highest in festival hours, and the WS had a far more significant influence on the NO₂ concentration than on the PM₁₀ concentration, indicating that pollutant concentrations in festival hours were mainly affected by local pollutant sources, which are closely related to vehicle exhausts and transport volumes. During workday hours, the influential extent of the WS on three pollutants was in equilibrium and pollutant concentrations were affected by local and exterior sources. Furthermore, pollutant concentrations that corresponded to orientation “NW to W” (8) in Figure 9a were far above average levels.

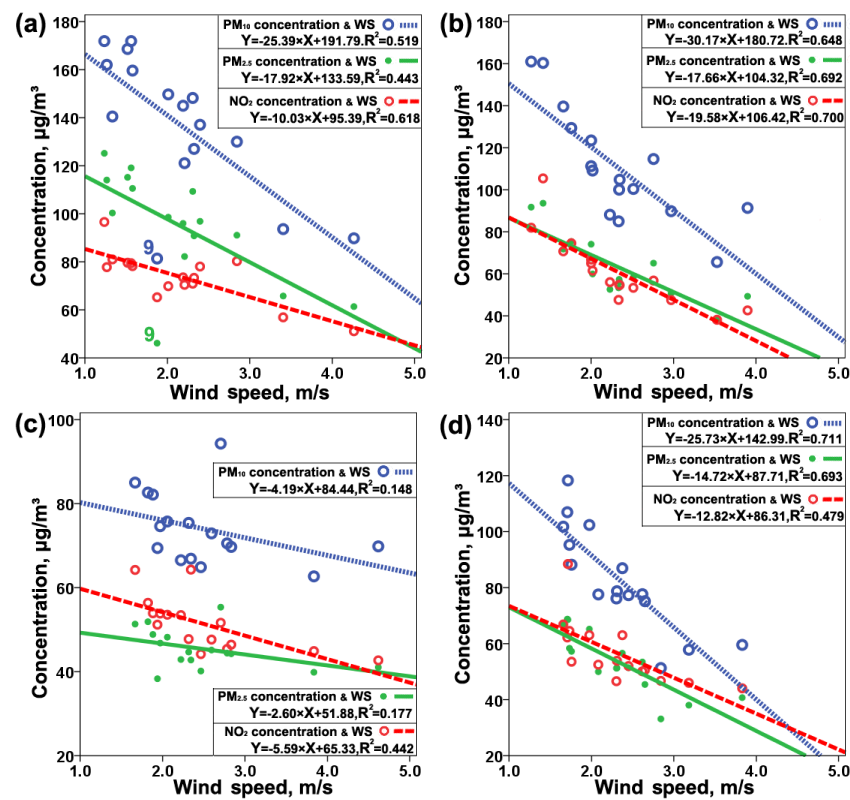


Figure 8. Influence of WS on pollutant concentrations over (a) winter, (b) spring, (c) summer and (d) autumn hours.

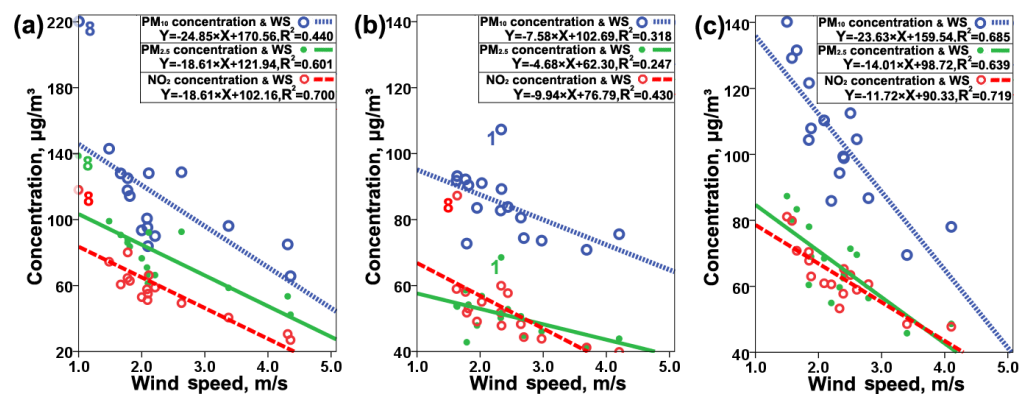


Figure 9. Influence of WS on pollutant concentrations over (a) festival, (b) TRD and (c) workday hours.

4. Discussion

By introducing the wind and spatial orientations in urban areas, analyses of orientation variations of the pollutant concentration can be further interpreted as comparisons of the air pollution status and pollutant dispersion in 16 orientations. The spatial orientation with heavy pollution can be analyzed by considering wind frequencies and social development status, and the cause of the heavy pollution can be attributed to either exterior sources or poor dispersions. During heavy pollution hours in four cycles, the WS had more significant influences on pollutant concentrations. Thus, diurnal peak hours, weekday hours, spring and autumn hours in the seasonal cycle, and workday and festival hours in the annual cycle were analyzed in this part, of which with linear R^2 between the WS and three pollutants above 0.6.

Figure 10 showed pollutant concentrations and the WS over diurnal peak hours, during which the WS prompted pollutant dispersions and introduced exterior sources. The

PM₁₀ and PM_{2.5} concentrations varied in consistency among 16 orientations, and obtained higher values in orientations 6, 7, 11, 12 and 13, and lower values in orientations 2, 3 and 4. By comparing the high pollution area with the “Chengdu Urban Master Plan (2011–2020)” and the current information on land use in Chengdu provided by the Chengdu municipal bureau of planning and natural resources, it can be found that the areas with the highest PM₁₀ and PM_{2.5} concentrations are precisely the areas with the highest construction density and industrial concentration in the city. Figure 10b shows the parcels of commercial and warehouse land in the city, which are mainly located in the orientation of 6, 7, 11, 12 and 13. Whereas orientations 6 and 7 face Pi county, the upstream (northwest of the Pidu district) of which is the Pengzhou petroleum plant, and the corresponding WS were below 1.5 m/s, hence both exterior sources and poor dispersion were the causes of the high pollutant concentration. orientation of 11, 12 and 13 have high wind frequencies but wind speeds below 1.8 m/s, suggesting that the higher building density in the area leads to lower wind speeds, resulting in poor dispersion and higher pollutant concentrations. While the NO₂ concentration varied with slight differences, and obtained higher values in orientations 8 and 16. Comparing the current urban land use situation, it can be seen that the orientation of 8 and 16 are located in the largest railway station area of the city, which is the distribution area of urban logistics and people flow, and the excessive traffic pressure is the reason for the high NO₂ in these two areas.

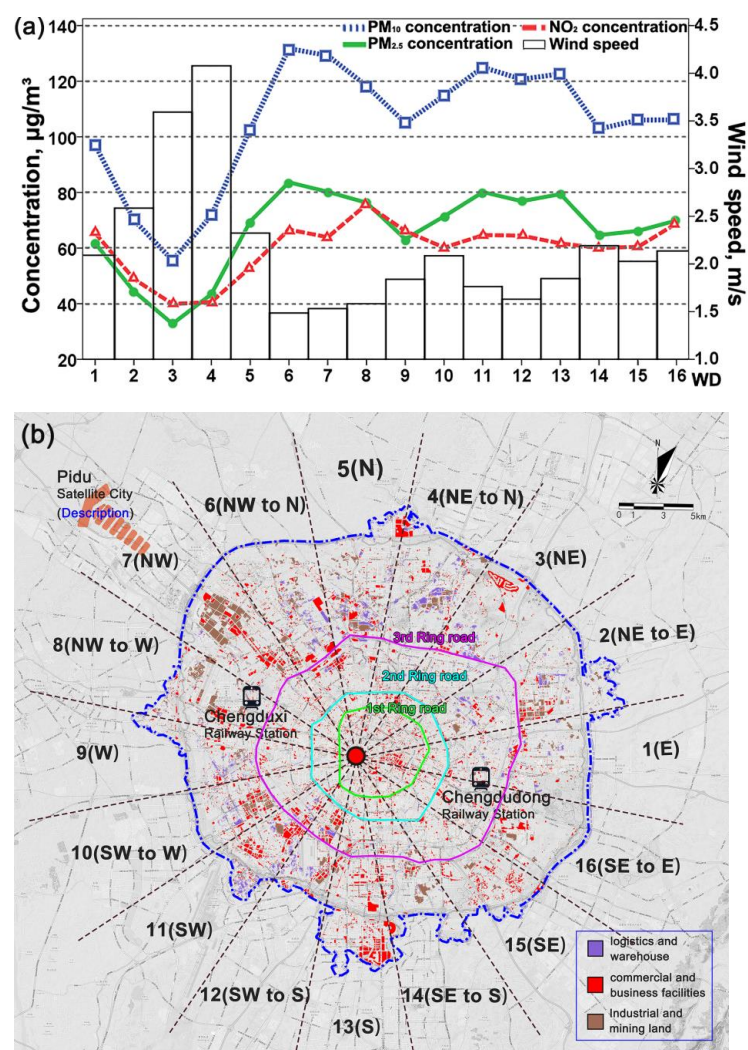


Figure 10. Pollutant concentrations and WS among 16 orientations: (a) over diurnal peak hours, with respect to (b) commercial and industrial land use planning map in Chengdu.

Figure 11 showed pollutant concentrations over weekday hours, which were affected by steady local and exterior sources. PM_{10} and NO_2 concentrations in orientation 8 were the highest among 16 orientations, because of the poor dispersion with low wind frequency and the corresponding WS was below 1.5 m/s. In addition, Wenjiang district, where the orientation 8 was facing, had no apparent sources both locally and exteriorly. As a traffic hub and a commercial land area, there are more traffic emission sources and higher building density in the orientation of 8, with low wind speeds, and this area was beyond the adjustable range of the local wind environment, and accumulated burdens from traffic related emissions might be the main cause of heavy pollution.

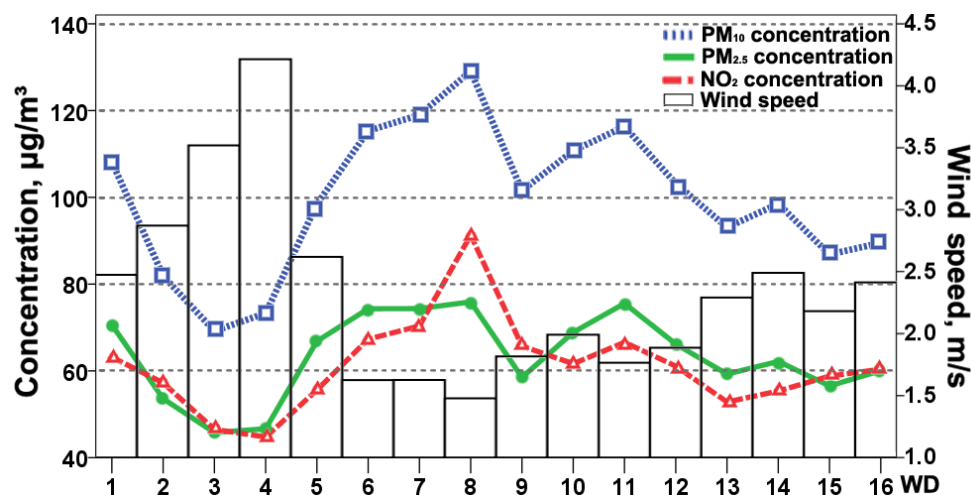


Figure 11. Pollutant concentrations and WS among 16 orientations over weekday hours.

Figure 12a,b shows pollutant concentrations and the WS over spring and autumn hours, and pollutant concentrations were higher over spring hours, and the pollution status over autumn hours was influenced by exterior sources remarkably. Three pollutants had higher values in orientations 7 and 8 over spring hours, and had higher values in orientations 6, 7, 8, 10 and 11 over autumn hours. Comparing the wind speed in spring and autumn, it can be found that the wind speed of 7 and 9 orientations in autumn is larger than the wind speed in spring. The pollutant concentration curves of 7 and 9 showed a decrease in the autumn when the wind speed was higher, indicating that the higher wind speed had a better pollutant dispersion effect in the same area.

Figure 13a,b shows pollutant concentrations and the WS over workday and festival hours, and the pollution status over festival hours was influenced by traffic related sources. Over workday hours, three pollutants had higher values in orientations 6, 7 and 8, and lower values in orientations 3 and 4. While over festival hours, the NO_2 concentration in the commercial land use areas, such as orientations 7 and 11, which are mainly office functions, showed a decrease. The NO_2 concentration in the orientation of 8 which is a railroad transportation hub, and the orientation 10 which is influenced by an air transport hub and Shuangliu traffic hub area, showed a rise. In particular, orientation 8 has the highest pollutant concentration, which is due to the low wind frequency and very low WS causing the poor dispersion of local emissions. However, it should be noted that the pollutant concentration in orientation 16, which is also a transportation hub, is lower than in orientation 8. The reason for this is that orientation 16 is in a centralized urban green area and has a lower building density, which makes the wind speed higher and effectively diffuses the pollutant sources. In addition, the dispersion effect of orientations 3 and 4 was excellent with apparently higher WS than above 4 m/s, which are the areas with the highest wind speed in each orientation, and with no apparent sources in the corresponding orientations, hence pollutant concentrations were the lowest over workday and festival hours.

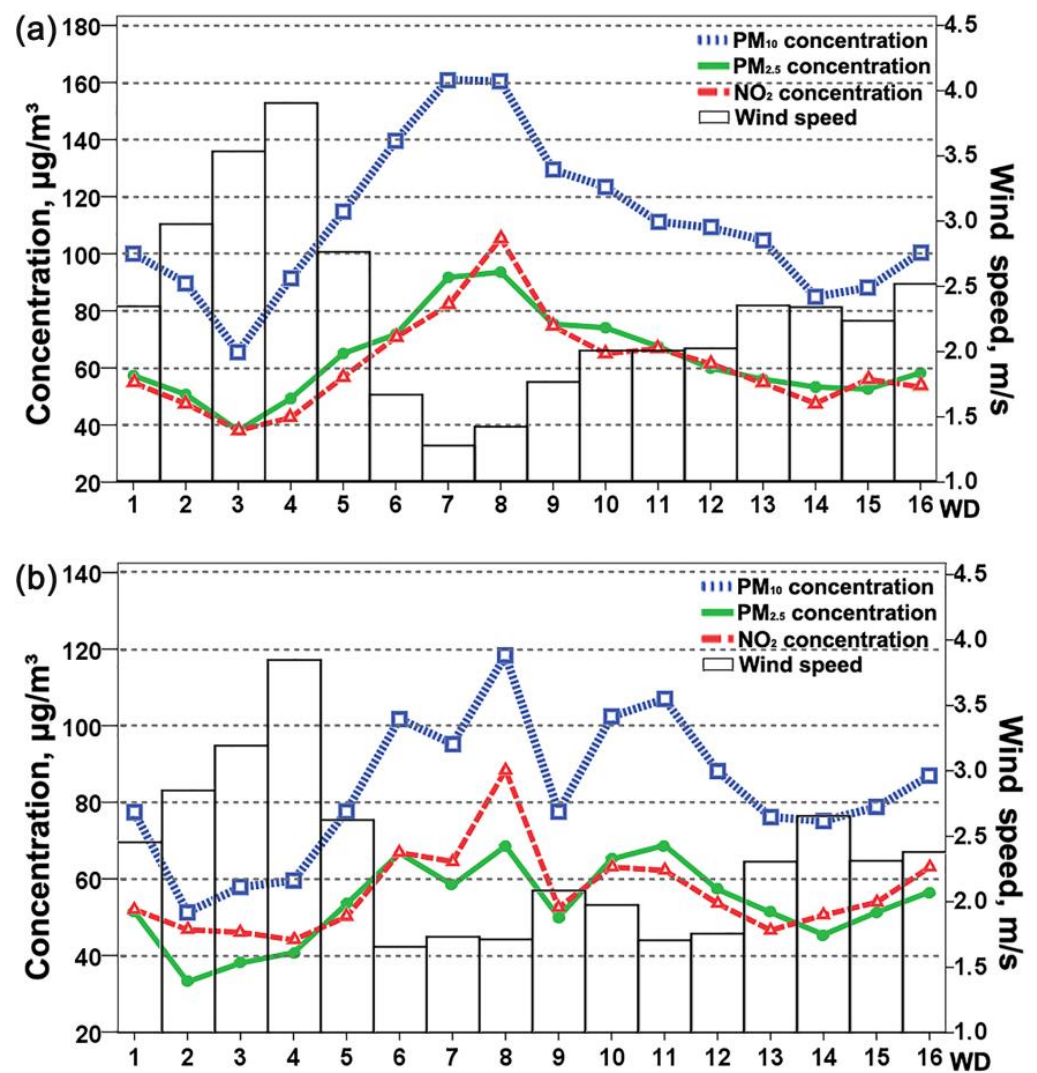


Figure 12. Pollutant concentrations and WS among 16 orientations over (a) spring and (b) autumn hours.

Over heavy pollution hours in diurnal, weekly, annual cycles and transitional seasons, the WS had more significant influences on pollutants, and whereas the wind frequency was not the main influencing factor for orientation variations. Comparisons among six time intervals in four cycles, the diffusion effect of orientations 2, 3 and 4 were excellent, with medium wind frequencies but exceptional high WS above 2.8 m/s, and wind panels to accelerate urban ventilation in these directions should be constructed. On the contrary, the wind in orientations 6, 7, 8, 11, 12 and 13 had a limited effect on pollutant dispersions, with the WS below 1.5 m/s generally and apt to be affected by local or exterior sources. The air pollution in orientation 8 (NW to N) was severe, and the pollution status in this area was beyond the adjustable range of the local wind environment.

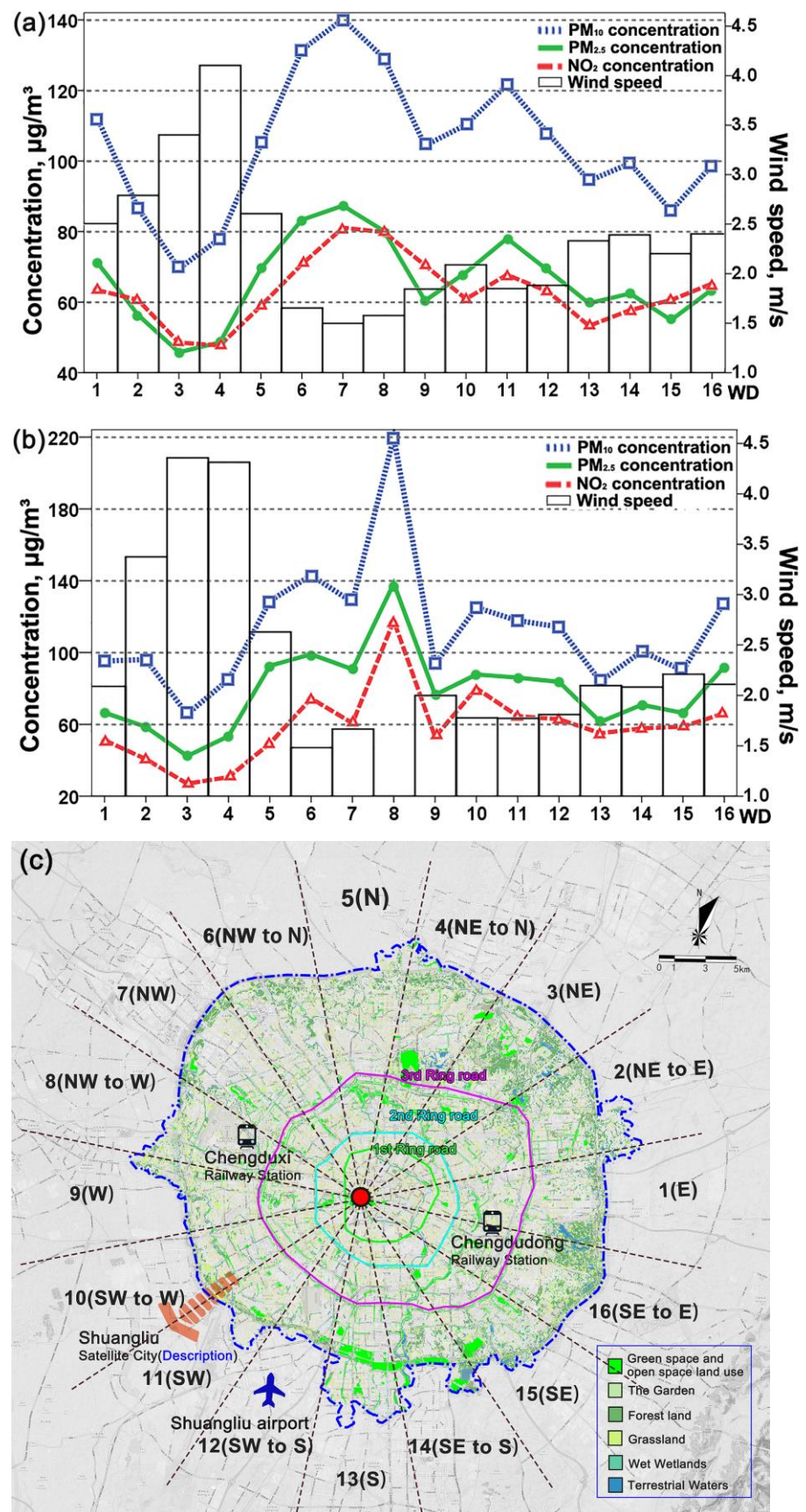


Figure 13. Pollutant concentrations and WS among 16 orientations over (a) workday and (b) festival hours, with respect to (c) green land use planning map in Chengdu.

5. Conclusions and Prospects

From the fluctuation patterns of the WS and three pollutants, the periodicity of diurnal, seasonal and annual cycles was remarkable, and the weekly cycle was obvious by adding the influence of the WS in 16 orientations. In the diurnal cycle, three pollutants had apparent valleys over off-peak hours, which may be concerned with higher WS and escalating temperature in the afternoon; and two peaks of the NO₂ concentration indicated the morning and evening travel rush hours, but had delays for 2 or 3 h. In the weekly cycle, NO₂ concentrations over weekend hours were lower than that over weekday hours, and the traffic volume on Monday increased after the decrement over the weekend. In the seasonal cycle, pollutant concentrations show that: winter hours > spring hours > autumn hours > summer hours, and obtained peak values in December and valley values in July. In the annual cycle, PM₁₀ and PM_{2.5} concentrations were the highest over festival hours, while NO₂ concentration was the highest over workday hours, and pollutant concentrations were the lowest over TRD hours for three pollutants. From the perspective of urban space and pollution concentrations, the areas with the highest PM₁₀ and PM_{2.5} concentrations show a high overlap with the concentrated areas of urban commercial and warehouse sites, where high building density leads to low wind speeds, resulting in poor dispersion and high pollutant concentrations. The areas with the highest NO₂ concentrations have a high overlap with areas where people and logistics are concentrated, such as urban transportation hubs like train stations and airports. In such areas, excessive traffic pressure and poor wind environment are the main causes of high NO₂ pollutant concentrations in cities. In addition, urban concentrated green areas have an effect on reducing the concentration of pollutants. In areas with low wind speed cities, planning urban concentrated green areas is an effective way to reduce the concentration of pollutants in local areas of the city.

During heavy pollution hours of diurnal, weekly, annual cycles and transitional seasons, WS had more significant influences on pollutants, and whereas wind frequency was not the main influencing factor for orientation variations. WS had direct impacts on pollutants when varied in the range of 1.5–2.5 m/s, and had remarkable diffusion effects on pollutants once above 2.5 m/s. In the diurnal cycle, as the WS prompted the diffusion of pollutants, exterior pollutant sources were also introduced. In the weekly cycle, pollutant sources showed discrepancies over weekday and weekend hours, by adding the influence of the WS on pollutants in 16 orientations. In the seasonal cycle, pollutant concentrations over spring hours were mainly affected by local pollutant sources, while the influence of the exterior pollutant source was significant over autumn hours. In the annual cycle, pollutant concentrations were mainly affected by local sources and vehicle exhausts. For Chengdu, the northeast orientation was suitable to construct a wind panel with a remarkable diffusion effect on pollutants, while air pollutions in the northwest and southwest orientations were severe with WS below 1.5 m/s, and pollution diffusion seems to be the worst in the north-northwest orientation.

The work at this stage initially makes a tentative effort to investigate the possible correlation between ambient air pollutants concentrations with city wind environment and distribution variations on different time scale considerations. When fitting and integrating the air pollutant concentration with climatic parameters, it will be affected by many other factors, such as atmospheric circulation, city size, physical-chemical properties of studied air pollutants, urban temperature, humidity and precipitation conditions, etc. Such limitations also arise in some future research works for further investigation:

- (1) An inland city with a monsoon climate, Chengdu, in western China is chosen as the case here, with a loop layout and central symmetry urban planning. Changes in climatic zones or regions (tropical, subtropical, maritime climates, etc.), terrain types (plain, plateau, mountain, coastal cities, etc.), and specific urban planning (commercial/industrial/residential districts, traffic network, etc.) can contribute to various air quality levels and distributions from different space and time scale perspectives.

- (2) Dynamic and coupled climatic conditions play a significant role in determining specific city outdoor air environments, in terms of dynamic temperature, humidity, precipitation and wind variation impacting both pollutants distribution and possible interactive reactions. The linear fitting approach is used here to approximately qualify the multi-impact city pollution distributions with climatic factor and time-scales considerations. More accurate and advanced algorithm or statistics analysis methods such as multiple regression, Fourier transformation, sequential quadratic programming, etc. might be more helpful to reveal explicitly the multi-factor interactive influence mechanism.
- (3) Practical city air quality index also depends on the pollutant types, monitoring and evaluation standards. For instance, the emission and transmission mechanisms are quite different among particles, volatile organic compounds and microorganism contaminants, resulting in different wind impacting effects. In practical applications, the air quality index could vary widely with different monitoring approaches, benchmarks and reference values, even in places or climatic regions.

Although the specific results obtained in typical cases may not meet all the situations under different conditions, the analysis methods used in this article, through quantitatively linking air pollutant concentrations with city wind distributions, are general and can be applied to other occasions. This work can provide analysis guidance and reference for urban planning optimization and city air quality control with wind-related climatic considerations, especially for those undergoing massive city expansion and infrastructure construction in developing countries.

Author Contributions: Conceptualization, J.X. and Y.Z.; methodology, Y.Z.; software, J.L. and F.G.; validation, J.L.; writing—original draft preparation, J.X.; writing—review and editing, J.L., F.G. and Y.Z.; supervision, Y.Z. All authors have read and agreed to the published version of the manuscript.

Funding: This work is supported by National Natural Science Foundation of China (No. 52108032) and Sichuan Science and Technology Research Program (No. 2022NSFSC1148).

Informed Consent Statement: Not applicable.

Data Availability Statement: For timely air quality index, main pollutant concentration and other climatic parameters, readers can visit the official website of Chengdu Ecological Environment Bureau (<http://sthj.chengdu.gov.cn>, accessed on 1 January 2022).

Conflicts of Interest: The authors declare no conflict of interest. The funders had no role in the design of the study, collection, analyses and decision to publish the results.

References

1. Zhou, Y.; Chen, Y.; Li, Z.L.; Jiang, W.L. Ecological resilience assessment of an emerging urban agglomeration: A case study of Chengdu-Chongqing economic circle, China. *Pol. J. Environ. Stud.* **2022**, *31*, 2381–2395.
2. Ouyang, H.L.; Tang, X.; Kumar, R.; Zhang, R.H.; Basseur, G.; Churchill, B.; Alam, M.; Kan, H.D.; Liao, H.; Zhu, T. Toward better and healthier air quality: Implementation of WHO 2021 global air quality guidelines in Asia. *Bull. Am. Meteorol. Soc.* **2022**, *103*, 1696–1703. [[CrossRef](#)]
3. Baklanov, A.; Molina, L.T.; Gauss, M. Megacities, air quality and climate. *Atmos. Environ.* **2016**, *126*, 235–249. [[CrossRef](#)]
4. Lu, D. Air pollution may be behind millions of deaths in China. *New Sci.* **2020**, *245*, 12. [[CrossRef](#)]
5. Iqbal, W.; Tang, Y.M.; Chau, K.Y.; Irfan, M.; Mohsin, M. Nexus between air pollution and NCOV-2019 in China: Application of negative binomial regression analysis. *Process Saf. Environ. Prot.* **2021**, *150*, 557–565. [[CrossRef](#)]
6. Wang, J.Y.; Gao, A.F.; Li, S.R.; Liu, Y.H.; Zhao, W.F.; Wang, P.; Zhang, H.L. Regional joint PM_{2.5}-O₃ control policy benefits further air quality improvement and human health protection in Beijing-Tianjin-Hebei and its surrounding areas. *J. Environ. Sci.* **2023**, *130*, 75–84. [[CrossRef](#)]
7. Hu, J.; Wang, Y.; Ying, Q.; Zhang, H. Spatial and temporal variability of PM_{2.5} and PM₁₀ over the North China Plain and the Yangtze River Delta, China. *Atmos. Environ.* **2014**, *95*, 598–609. [[CrossRef](#)]
8. Tian, Y.Z.; Shi, G.L.; Han, B.; Wu, J.H.; Zhou, X.Y.; Zhou, L.D.; Zhang, P.; Feng, Y.C. Using an improved Source Directional Apportionment method to quantify the PM_{2.5} source contributions from various directions in a megacity in China. *Chemosphere* **2015**, *119*, 750–756. [[CrossRef](#)] [[PubMed](#)]
9. Chen, Y.; Xie, S.D. Characteristics and formation mechanism of a heavy air pollution episode caused by biomass burning in Chengdu, Southwest China. *Sci. Total Environ.* **2014**, *473–474*, 507–517. [[CrossRef](#)]

10. Chu, H.J.; Huang, B.; Lin, C.Y. Modeling the spatio-temporal heterogeneity in the PM₁₀-PM_{2.5} relationship. *Atmos. Environ.* **2015**, *102*, 176–182. [[CrossRef](#)]
11. Hai, C.D.; Kim Oanh, N.T. Effects of local, regional meteorology and emission sources on mass and compositions of particulate matter in Hanoi. *Atmos. Environ.* **2013**, *78*, 105–112. [[CrossRef](#)]
12. Yin, Z.C.; Li, Y.Y.; Zhang, Y.J.; Wang, H.J. Evident differences of haze days between December and January in north China and possible relationships with preceding climate factors. *Int. J. Climatol.* **2023**, *43*, 438–455. [[CrossRef](#)]
13. Chen, Y.; Luo, B.; Xie, S.D. Characteristics of the long-range transport dust events in Chengdu, Southwest China. *Atmos. Environ.* **2015**, *122*, 713–722. [[CrossRef](#)]
14. Shi, G.L.; Liu, J.Y.; Tian, Y.Z.; Song, D.L.; Yu, H.F.; Feng, Y.C.; Russell, A.G. Quantification of long-term primary and secondary source contributions to carbonaceous aerosols. *Environ. Pollut.* **2016**, *219*, 897–905. [[CrossRef](#)] [[PubMed](#)]
15. Wang, J.; Li, J.; Li, X.L.; Fang, C.S. Characteristics of Air Pollutants Emission and Its Impacts on Public Health of Chengdu, Western China. *Int. J. Environ. Res. Public Health* **2022**, *19*, 16852. [[CrossRef](#)]
16. Zhou, Z.H.; Tan, Q.W.; Liu, H.F.; Deng, Y.; Wu, K.Y.; Liu, C.W.; Zhou, X.L. Emission characteristics and high-resolution spatial and temporal distribution of pollutants from motor vehicles in Chengdu, China. *Atmos. Pollut. Res.* **2019**, *10*, 749–758. [[CrossRef](#)]
17. Hu, H.; Zeng, S.L.; Han, X. Effects of Urban Landscapes on Pollutant Concentrations in Chengdu Plain Urban Agglomeration. *Atmosphere* **2022**, *13*, 1492. [[CrossRef](#)]
18. Wang, H.F.; Liu, Z.H.; Zhang, Y.; Yu, Z.Y.; Chen, C.R. Impact of different urban canopy models on air quality simulation in Chengdu, southwestern China. *Atmos. Environ.* **2021**, *267*, 118775. [[CrossRef](#)]
19. Sun, W.; Liu, Z.H.; Zhang, Y.; Xu, W.X.; Lv, X.T.; Liu, Y.Y.; Li, X.; Xiao, J.; Ma, F. Study on Land-use Changes and Their Impacts on Air Pollution in Chengdu. *Atmosphere* **2020**, *11*, 42. [[CrossRef](#)]
20. Li, Y.; Chen, Q.; Zhao, H.; Wang, L.; Tao, R. Variations in PM₁₀, PM_{2.5} and PM_{1.0} in an urban area of the Sichuan Basin and their relation to meteorological factors. *Atmosphere* **2015**, *6*, 150–163. [[CrossRef](#)]
21. Chen, Z.G.; Chen, C.; Wei, S.; Wu, Y.Q.; Wang, Y.F.; Wan, Y.L. Impact of the external window crack structure on indoor PM_{2.5} mass concentration. *Build. Environ.* **2016**, *108*, 240–251. [[CrossRef](#)]
22. Gomez-Carracedo, M.P.; Andrade, J.M.; Ballabio, D.; Prada-Rodriguez, D.; Muniategui-Lorenzo, S.; Consonni, V.; Pineiro-Iglesias, M.; Lopez-Mahia, P. Impact of medium-distance pollution sources in a Galician suburban site (NW Iberian peninsula). *Sci. Total Environ.* **2015**, *512–513*, 114–124. [[CrossRef](#)] [[PubMed](#)]
23. Grundström, M.; Hak, C.; Chen, D.; Hallquist, M.; Pleijel, H. Variation and co-variation of PM₁₀, particle number concentration, NO_x and NO₂ in the urban air—Relationships with wind speed, vertical temperature gradient and weather type. *Atmos. Environ.* **2015**, *120*, 317–327. [[CrossRef](#)]
24. Squizzato, S.; Masiol, M. Application of meteorology-based methods to determine local and external contributions to particulate matter pollution: A case study in Venice (Italy). *Atmos. Environ.* **2015**, *119*, 69–81. [[CrossRef](#)]
25. Uria-Tellaetxe, I.; Carslaw, D.C. Conditional bivariate probability function for source identification. *Environ. Model. Softw.* **2014**, *59*, 1–9. [[CrossRef](#)]
26. Salazar, A.A.; Zheng, J.F.; Che, Y.Z.; Xiao, F. Deep generative model for probabilistic wind speed and wind power estimation at a wind farm. *Energy Sci. Eng.* **2022**, *10*, 1855–1873. [[CrossRef](#)]
27. Zeng, Y.Y.; Jaffe, D.A.; Qiao, X.; Miao, Y.C.; Tang, Y. Prediction of potentially high PM_{2.5} concentrations in Chengdu, China. *Aerosol Air Qual. Res.* **2020**, *20*, 956–965. [[CrossRef](#)]
28. Xie, J.L.; Sun, T.L.; Liu, C.F.; Li, L.; Xu, X.Q.; Miao, S.J.; Lin, L.H.; Chen, Y.Y.; Fan, S.J. Quantitative evaluation of impacts of the steadiness and duration of urban surface wind patterns on air quality. *Sci. Total Environ.* **2022**, *850*, 157957. [[CrossRef](#)] [[PubMed](#)]
29. Rashidi, R.; Khaniabadi, Y.O.; Sicard, P.; De Marco, A.; Anbari, K. Ambient PM_{2.5} and O₃ pollution and health impacts in Iranian megacity. *Stoch. Environ. Res. Risk Assess.* **2022**, *37*, 175–184. [[CrossRef](#)]
30. Xiang, J.B.; Seto, E.; Mo, J.H.; Zhang, J.F.; Zhang, Y.P. Impacts of implementing Healthy Building guidelines for daily PM_{2.5} limit on premature deaths and economic losses in urban China: A population-based modeling study. *Environ. Int.* **2021**, *147*, 106342. [[CrossRef](#)]
31. Xiang, J.B.; Weschler, C.J.; Wang, Q.Q.; Zhang, L.; Mo, J.H.; Ma, R.; Zhang, J.F.; Zhang, Y.P. Reducing indoor levels of outdoor PM_{2.5} in urban China: Impact on mortalities. *Environ. Sci. Technol.* **2021**, *53*, 3119–3127. [[CrossRef](#)] [[PubMed](#)]

Disclaimer/Publisher’s Note: The statements, opinions and data contained in all publications are solely those of the individual author(s) and contributor(s) and not of MDPI and/or the editor(s). MDPI and/or the editor(s) disclaim responsibility for any injury to people or property resulting from any ideas, methods, instructions or products referred to in the content.